On the local stability condition in the planar beam finite element

Igor Planinc[†], Miran Saje[‡] and Bojan Čas[‡†]

Faculty of Civil and Geodetic Engineering, University of Ljubljana, Jamova 2, SI-1115 Ljubljana, Slovenia

Abstract. In standard finite element algorithms, the local stability conditions are not accounted for in the formulation of the tangent stiffness matrix. As a result, the loss of the local stability is not adequately related to the onset of the global instability. The phenomenon typically arises with material-type localizations, such as shear bands and plastic hinges. This paper addresses the problem in the context of the planar, finite-strain, rate-independent, materially non-linear beam theory, although the proposed technology is in principle not limited to beam structures. A weak formulation of Reissner's finite-strain beam theory is first presented, where the pseudocurvature of the deformed axis is the only unknown function. We further derive the local stability conditions for the large deformation case, and suggest various possible combinations of the interpolation and numerical integration schemes that trigger the simultaneous loss of the local and global instabilities of a statically determined beam. For practical applications, we advice on a procedure that uses a special numerical integration rule, where interpolation nodes and integration points are equal in number, but not in locations, except for the point of the local instability, where the interpolation node and the integration point coalesce. Provided that the point of instability is an end-point of the beam– a condition often met in engineering practice–the procedure simplifies substantially; one of such algorithms uses the combination of the Lagrangian interpolation and Lobatto's integration. The present paper uses the Galerkin finite element discretization, but a conceptually similar technology could be extended to other discretization methods.

Key words: local stability; planar beam; finite element; numerical integration; plasticity.

1. Introduction

Loss of stability is a common phenomenon in the nonlinear mechanics of solids and structures. Typical examples are the buckling of a rod, the necking of a bar due to tension, and the localization of deformed shear bands. In stability analyses, we have to distinguish between global and local instabilities. The objective of the present paper is to set up a procedure that, in a context of a finite element analysis of planar materially and geometrically nonlinear beams, consistently relates the loss of the local stability in an element with the global instability of the structure.

In standard finite element formulations, the emergence of the local instability is not automatically accounted for in the tangent stiffness matrix. Consequently, the loss of the local stability within a finite element is not correctly related to the deterioration of the bearing capacity of a structure, and, in particular, to the possible loss of its global stability. This kind of instability is typically–but not

---

only-associated with materially driven strain localizations in ductile solids, such as shear bands and plastic hinges (see the original works by Ortiz *et al.* 1987 and Belytschko *et al.* (1988) for the description of the phenomenon and their proposals leading to an enhanced performance of the finite element method). It appears, however, that the issue here termed the 'consistent consideration of local stability conditions in the stiffness matrix', has not received an adequate attention in the finite element literature. This lack of interest is in sharp contrast with the activities aiming at the deduction of methods for the computation of global instability points, which are now relatively well developed, see, Crisfield (1991) for an overview of the methods, and Wriggers *et al.* (1988), Wriggers and Simo (1990), Fujii and Okazawa (1997) and Planinc and Saje (1998).

   The starting point of our study is Reissner's (1972) finite-strain planar beam theory. Several variational, weak-form settings are possible for Reissner's theory for their finite element implementations (Saje *et al.* 1997). To facilitate the derivation of the local stability conditions in a beam, we first shortly describe a variational formulation of Reissner's beam where the pseudocurvature of the deformed axis of a beam plays the role of the fundamental unknown function. Then we derive the set of local stability conditions of a beam and study how these conditions can be incorporated into the tangent stiffness matrix of a finite element so that the onset of the local instability triggers the simultaneous loss of the global stability of a beam. The discussion that follows shows that these conditions can be satisfied indeed, provided that the positions of the interpolation points and the integration algorithm satisfy certain requirements. This is described in Section 4 in detail. Our discussion was inspired by the work of Banovec (1986) on the moderate-strain, large displacement, large rotation, co-rotational, mixed-energy based finite element formulation of elastic-plastic planar beams, in which the transverse displacement is the fundamental unknown function. Based on the small-strain material stability conditions, he proved that the number of interpolation nodes for the transverse displacements and the number of integration points must be equal for the local stability to be consistently captured in the tangent stiffness matrix of an element. We interpret our work as an extension and generalization, in a systematic way, of that carried out by Banovec (1986), to include large deformations.

2. Formulation of basic equations

2.1 Kinematic and constitutive equations

   We consider an initially straight, planar, materially non-linear beam of undeformed length L and of constant cross-section A. The beam is analyzed in the (X, Z)-plane of a fixed-in-space Cartesian coordinate system (X, Y, Z) with orthonormal base vectors E_X, E_Y, E_Z, where $E_Y = E_Z \times E_X$. Without a loss of generality and for the sake of simplicity, we assume that the centroid axis of the beam initially coincides with the X axis. The shape of the cross-section of the beam, and material distribution over the cross-section are assumed to be symmetric with respect to plane (X, Z), but otherwise arbitrary. A material particle of the beam is identified by material coordinates $x \in [0, L]$, $(y, z) \in A$, coinciding with coordinates X, Y, Z in the undeformed state. The centroid axis is identified by $y = z = 0$. Extensional, bending, and shear strains are assumed to take part in the deformation of the beam, but Bernoulli's hypothesis of planar and undistorted cross-sections is only considered. The beam is subjected to the action of distributed loads $p_x(x)$, $p_z(x)$, and distributed moment load $m_y(x)$ along its span and to concentrated generalized forces S_i ($i = 1, 2, \cdots, 6$) at its ends; p_x and p_z

are the components of the distributed load vector with regard to base vectors $\boldsymbol{E}_X$ and $\boldsymbol{E}_Z$. The loading is assumed to be deformation-independent.

A deformed configuration of the centroid axis of the beam is defined by a vector-valued function

$$\boldsymbol{r}(x) = (x + u(x))\boldsymbol{E}_X + w(x)\boldsymbol{E}_Z, \tag{1}$$

where $u(x)$ and $w(x)$ are the components of the displacement vector of the centroid axis with respect to base vectors $\boldsymbol{E}_X$ and $\boldsymbol{E}_Z$, respectively.

The components of the displacement vector are related to geometrical and deformation variables of the beam by the equations derived by Reissner (1972):

$$1 + u' - (1 + \varepsilon)\cos\varphi - \gamma\sin\varphi = 0, \tag{2}$$

$$w' + (1 + \varepsilon)\sin\varphi - \gamma\cos\varphi = 0, \tag{3}$$

$$\varphi' - k = 0. \tag{4}$$

In Eqs. (2)-(4) the prime (′) denotes the derivative with respect to x, whereas functions $\varepsilon(x) > -1$, $\gamma(x)$, $\varphi(x)$, and $\kappa(x)$ mark the extensional strain (i.e., the specific elongation), the shear strain, the rotation, and the pseudocurvature of the centroid axis, respectively. Functions u, w, and φ will here be termed the *geometrical variables*, as they determine the geometrical configuration space of the beam. Functions ε, γ, and κ, i.e., the generalized strains of the beam, span the *deformation configuration space* (superposed to the rigid displacements) and will, therefore, be termed the deformation variables. Observe that κ coincides with the actual curvature of the deformed centroid axis of the beam only when $\varepsilon = \gamma = 0$; thus, the term 'pseudocurvature' is appropriate. The extensional strain of an arbitrary material particle (x, y, z) of the beam is denoted by e and is determined by Bernoulli's hypothesis-based relation

$$e(x, z) = \varepsilon(x) + z\kappa(x). \tag{5}$$

In order to relate equilibrium axial and shear forces, $\mathcal{N}$ and $\mathcal{Q}$, and *equilibrium* moment $\mathcal{M}$ to a material model, we introduce the set of constitutive equations which assures the balance of the equilibrium and constitutive cross-sectional forces, Antman and Rosenfeld (1978)

$$\mathcal{N}(x) = \mathcal{N}_c\left(\varepsilon(x),\ \gamma(x),\ \kappa(x)\right), \tag{6}$$

$$\mathcal{Q}(x) = \mathcal{Q}_c\left(\varepsilon(x),\ \gamma(x),\ \kappa(x)\right), \tag{7}$$

$$\mathcal{M}(x) = \mathcal{M}_c\left(\varepsilon(x),\ \gamma(x),\ \kappa(x)\right). \tag{8}$$

Constitutive functions $\mathcal{N}_c$, $\mathcal{Q}_c$, and $\mathcal{M}_c$ are defined as cross-sectional true stress resultants, and are termed the *constitutive axial* and *shear forces* and the *constitutive bending moment*, respectively. The constitutive functions are subordinate to the adopted material constitutive model, which is, in our case, defined by the normal true stress-strain law given by the generic relation $\sigma_c = \mathcal{F}(e)$, and by the shear stress-strain law $\tau_c = \mathcal{G}(\gamma)$ which will be defined later; here $\mathcal{F}$ and $\mathcal{G}$ designate functions appropriate for material to be considered. These relationships describe a broad set of materials, including hyperelastic, and elastic-plastic ones. In terms of stresses, the constitutive functions are given by the equations

$$\mathcal{N}_c(\varepsilon,\ \gamma,\ \kappa) = \int_A \sigma_c(x, y, z)\, dA, \tag{9}$$

$$\mathcal{Q}_c(\varepsilon,\, \gamma,\, \kappa)=\int_A \tau_c(x,\, y,\, z)dA=GA_s\gamma(x)\,, \tag{10}$$

$$\mathcal{M}_c(\varepsilon,\, \gamma,\, \kappa)=\int_A z\sigma_c(x,\, y,\, z)dA\,. \tag{11}$$

A simple constitutive model for the shear strain is adopted here, so that $\mathcal{Q}_c=GA_s\gamma$; $G(\gamma)$ is the shear strain-dependent tangent shear modulus of material, and $0<A_s<A$ is the area of the shear cross-section (Cowper 1966).

2.2 The modified principle of virtual work and its finite element formulation

The principle of virtual work states that the difference of virtual work of internal and external forces is zero (Washizu 1981)

$$\int_0^L (\mathcal{N}\delta\varepsilon + \mathcal{Q}\delta\gamma + \mathcal{M}\delta\kappa)dx - \int_0^L (p_x\delta u + p_z\delta w + m_y\delta\varphi)dx - \sum_{i=1}^6 S_i\delta u_i=0. \tag{12}$$

Here, δu, δw, and $\delta\varphi$ are virtual displacements and rotation, and $\delta\varepsilon$, $\delta\gamma$, $\delta\kappa$ are virtual strains of the centroid axis; δu_i ($i = 1, 2, \cdots, 6$) denote the generalized virtual boundary displacements such that

$$\delta u_1 = \delta u\,(0), \quad \delta u_2 = \delta w\,(0), \quad \delta u_3 = \delta\varphi\,(0),$$

$$\delta u_4 = \delta u\,(L), \quad \delta u_5 = \delta w\,(L), \quad \delta u_6 = \delta\varphi\,(L).$$

In (12) the deformation geometrical variables as well as their variations must satisfy the three kinematic Eqs. (2)–(4). Thus, only three among the six functions u, w, φ, ε, γ, and κ are mutually independent. A common practice is to express the deformation variables in terms of the geometrical ones, $\varepsilon=\varepsilon\,(u',\, w',\, \varphi)$, $\gamma=\gamma\,(u',\, w',\, \varphi)$, $\kappa=\varphi'$ (2)–(4); then by inserting these expressions into the constitutive relations Eqs. (9)-(11) and after employing Eqs. (6)–(8) in (12), one obtains the displacement-based principle of virtual work. Disadvantages of a such formulation are well known in the finite element literature (see, e.g., the comprehensive book by Crisfield 1991, 1997). In contrast to the displacement-based formulation, the present study relies on the deformation variables as basic unknowns of the problem. Such a deformation-based formulation offers a number of advantages, two of which are more transparent local stability criteria discussed later on in the paper, and a consistent cross-section equilibrium.

The starting point of the deformation-based Galerkin-type of the finite element discretization method is the modified principle of virtual work (Planinc 1998)

$$\int_0^L (\mathcal{M}_c - \mathcal{M})\,\delta\kappa dx$$

$$+\Big(u(L)-u(0)-\int_0^L [(1 + \varepsilon)\cos\varphi+ \gamma\sin\varphi]dx+L \Big)\delta\mathcal{R}_1(0)$$

$$+\Big(w(L)-w(0)+\int_0^L [(1 + \varepsilon)\sin\varphi- \gamma\cos\varphi]dx \Big)\delta\mathcal{R}_2(0)$$

$$+\Big(\varphi(L)-\varphi(0) - \int_0^L \kappa dx \Big)\delta\mathcal{M}(0)$$

$$-[S_1+\mathcal{R}_1(0)]\delta u_1-[S_2+\mathcal{R}_2(0)]\delta u_2-[S_3+\mathcal{M}(0)]\delta u_3$$

$$-[S_4-\mathcal{R}_1(L)]\delta u_4- [S_5-\mathcal{R}_2(L)]\delta u_5 - [S_6-\mathcal{M}(L)]\delta u_6=0\,. \tag{14}$$

The only function defining the principle given above is the deformation variable–the pseudocurvature $\kappa(x)$; note that the geometrical and force variables are included only through their boundary values $u(0)$, $w(0)$, $\varphi(0)$, $u(L)$, $w(L)$, $\varphi(L)$, $\mathcal{R}_1(0)$, $\mathcal{R}_2(0)$, and $\mathcal{M}(0)$. Function $\kappa(x)$ and nine parameters $(\mathcal{R}_1(0)$, $\mathcal{R}_2(0)$, $\mathcal{M}(0)$, $u(0)$, $w(0)$, $\varphi(0)$, $u(L)$, $w(L)$, $\varphi(L))$ fully describe the principle (14). For the approximation of pseudocurvature $\kappa(x)$ along a finite element, Lagrangian polynomials $P_n(x)$ ($n = 1, 2, \cdots, N$) of degree $N{-}1$ are used. N-node mesh is applied with the end points of the element being the first and the last node, respectively. The distribution of the pseudocurvature along the element axis is represented by the interpolation equation:

$$\kappa(x) = \sum_{n=1}^{N} P_n(x)\kappa_n. \tag{15}$$

After the introduction of (15) into (14) we get the following discrete system of the equilibrium equations of the planar beam (Planinc 1998):

$$g_n = \int_0^L (\mathcal{M}_c - \mathcal{M}) P_n dx = 0, \quad n = 1, 2, \ldots, N, \tag{16}$$

$$g_{N+1} = u(L) - u(0) - \int_0^L [(1 + \varepsilon)\cos\varphi + \gamma\sin\varphi] dx + L = 0, \tag{17}$$

$$g_{N+2} = w(L) - w(0) + \int_0^L [(1 + \varepsilon)\sin\varphi - \gamma\cos\varphi] dx = 0, \tag{18}$$

$$g_{N+3} = \varphi(L) - \varphi(0) - \sum_{n=1}^{N} P_n^*(L)\kappa_n = 0, \tag{19}$$

$$g_{N+4} = S_1 + \mathcal{R}_1(0) = 0, \tag{20}$$

$$g_{N+5} = S_2 + \mathcal{R}_2(0) = 0, \tag{21}$$

$$g_{N+6} = S_3 + \mathcal{M}(0) = 0, \tag{22}$$

$$g_{N+7} = S_4 - \mathcal{R}_1(0) + \int_0^L p_x dx = 0, \tag{23}$$

$$g_{N+8} = S_5 - \mathcal{R}_2(0) + \int_0^L p_z dx = 0, \tag{24}$$

$$g_{N+9} = S_6 - \mathcal{M}(0) - \int_0^L [(1 + \varepsilon)\mathcal{Q} - \gamma\mathcal{N} - m_y] dx = 0, \tag{25}$$

in which $\mathcal{N} = \mathcal{R}_1\cos\varphi - \mathcal{R}_2\sin\varphi$, $\mathcal{Q} = \mathcal{R}_1\sin\varphi + \mathcal{R}_2\cos\varphi$ are the equilibrium axial and shear forces, respectively, and

$$\mathcal{M}(x) = \mathcal{M}(0) + \int_0^x [(1 + \varepsilon)\mathcal{Q} - \gamma\mathcal{N} - m_y] d\xi \tag{26}$$

is the equilibrium bending moment. Functions $\mathcal{M}_c$, ε, and γ are determined from Eqs. (11), (6), and (7), respectively.

Eqs. (16)–(25) constitute the system of $N + 9$ nonlinear equations for the determination of $N + 9$ degrees of freedom, i.e., $N + 3$ internal, κ_n ($n = 1, 2, \cdots, N$), $\mathcal{R}_1(0)$, $\mathcal{R}_2(0)$, $\mathcal{M}(0)$, and six external degrees of freedom, $u(0)$, $w(0)$, $\varphi(0)$, $u(L)$, $w(L)$, $\varphi(L)$, of the beam finite element. In the matrix form, these equations read

$$\boldsymbol{g}(\boldsymbol{x}, \lambda) = \boldsymbol{R}(\boldsymbol{x}) - \boldsymbol{P} = \boldsymbol{R}(\boldsymbol{x}) - \lambda\bar{\boldsymbol{P}} = \boldsymbol{0}. \tag{27}$$

Here, x denotes the $(N + 9)$-dimensional generalized displacement vector, R is the corresponding internal force vector, $P = \lambda \bar{P}$ is the deformation independent vector of external loads, $\bar{P}$ is a reference load vector, while λ is a loading factor. Formally a fully analogous equation is valid for an element assemblage–a planar frame.

Because internal degrees of freedom κ_n $(n = 1, 2, \cdots, N)$, $\mathcal{R}_1(0)$, $\mathcal{R}_2(0)$, and $\mathcal{M}(0)$ need not be continuous across the boundaries of the element, they may (but not necessarily) be eliminated from Eqs. (16)–(25) on an element level; the finite element equation then takes a similar form as in Eq. (27)

$$g_b(x_b, \lambda) = R_b(x_b) - \lambda \bar{P}_b = 0 . \tag{28}$$

Here, x_b denotes the vector of generalized boundary displacements, $u(0)$, $w(0)$, $\varphi(0)$, $u(L)$, $w(L)$, $\varphi(L)$, and R_b, $\bar{P}_b$ are the corresponding internal and external force vectors.

For a prescribed loading factor, $\lambda = \lambda_p$, and for prescribed boundary conditions, the system of equations given by (27) and assembled for the whole structure is solved for $x(\lambda_p)$ by Newton's iterative method. In an iteration step $i + 1$, Eq. (27) is linearized around the solution vector in iteration step i, yielding a system of linear equations for increments of unknowns

$$\nabla_x g(x_i, \lambda_p) \Delta x_{i+1} = -g(x_i, \lambda_p) ,$$
$$x_{i+1} = x_i + \Delta x_{i+1} \quad (i = 0, 1, 2, \dots) , \tag{29}$$

which is repeatedly solved until the required accuracy of x is achieved. The expression

$$\nabla_x g(x_i, \lambda_p) \Delta x_{i+1} = \frac{d}{d\alpha} [g(x_i + \alpha \Delta x_{i+1}, \lambda_p)] \Big|_{\alpha=0} \tag{30}$$

denotes the directional differential (Hughes and Pister 1978). The associated Fréchet's derivative $K_T \equiv \nabla_x g$ is, in the mechanics context, termed the tangent *stiffness matrix*. The definiteness of the tangent stiffness matrix of an element plays a crucial role in the local and global stability analyses, as discussed in the next section.

3. Singular points and local stability criteria

3.1 Preliminaries

The solution $x(\lambda)$ of Eq. (27) may be imagined as a continuous collection of points of the equilibrium of the structure in its displacement configuration space. In general, we distinguish between regular and singular points. Regular points are characterized by the regular tangent stiffness matrix (det $K_T \neq 0$). In a singular point, the matrix is singular:

$$\text{singular point} \Leftrightarrow \det K_T(x_{cr}, \lambda_{cr}) = 0. \tag{31}$$

The corresponding generalized displacement vector and loading factor in the singular point are called the critical displacement vector and the critical loading factor, respectively, and are denoted by x_{cr} and λ_{cr}. According to the implicit function theorem, Eq. (27) need not be uniquely solved for x in the singular point. The singular point, therefore, indicates a possible loss of uniqueness of the solution.

The points may further be divided into stable and unstable. For deformation-independent external loads considered here, the stable point is characterized by the positive definite tangent stiffness

matrix, i.e., by the condition (Waszczyszyn *et al.* 1994)

$$\boldsymbol{y}^t \boldsymbol{K}_T \boldsymbol{y} > 0, \quad \text{for all } \boldsymbol{y} \neq 0. \tag{32}$$

In (32), $(\cdot)^t$ denotes the transpose operation. Necessary and sufficient conditions for the positive definiteness of a matrix are well known (see, e.g., Hohn 1973 and Ting 1996). For any matrix, $\boldsymbol{M}$, the relation $\boldsymbol{y}^t \boldsymbol{M} \boldsymbol{y} = \boldsymbol{y}^t \boldsymbol{M}_s \boldsymbol{y}$ holds true, where $\boldsymbol{M}_s = 1/2(\boldsymbol{M} + \boldsymbol{M}^t)$ is the symmetric part of $\boldsymbol{M}$. Therefore, for a matrix to be positive definite, the leading principle minors of its symmetric part, $\boldsymbol{M}_s$, have to be positive. If matrix $\boldsymbol{M}_s$ is singular or negative definite, the point is unstable. In the engineering terminology, we call a structure having singular or negative definite symmetrized tangent global stiffness matrix to be *unstable*.

As the determinants of a matrix and its symmetric part are generally not equal, the stability and uniqueness criteria for non-symmetric stiffness matrices are not coincidental. Thus, a singular point of a structure, characterized by det $\boldsymbol{K}_T = 0$, may be stable or unstable, depending on the definiteness of the symmetric matrix $1/2(\boldsymbol{K}_T + \boldsymbol{K}_T^t)$. For a symmetric matrix, its singularity indicates both the loss of stability and the loss of uniqueness. Regular points may generally be stable or unstable for any type of the stiffness matrix (de Borst *et al.* 1993), too.

We further distinguish between *global* and *local* instabilities. The term 'global instability' describes the instability (in the sense defined above) of the whole structure, while the term 'local instability' indicates instability of a material point of a body. The two types of instabilities are only indirectly related; i.e., the local instability may or may not instantaneously trigger the global instability, yet it may well quantitatively change the global stiffness of the structure. It is, therefore, of the utmost importance to incorporate the onset of local instabilities into the global analysis. The aim of the present paper is to derive the algorithm that accounts for the effect of the local instability onto the global stiffness matrix in the context of Galerkin's beam finite element method and to present the conditions that the local instability sets to numerical integration schemes. However prior to the relevant discussions, we, have to deduce the local stability criteria for the beam.

3.2 Local stability criteria for the beam

Making use of (26) in (8), one obtains

$$r_3 = \mathcal{M}_c - \mathcal{M}(0) - \int_0^x \left[(1 + \varepsilon)\mathcal{Q} - \gamma \mathcal{N} - m_y \right] d\xi = 0. \tag{33}$$

Eqs. (6)−(7) and (33) relate equilibrium and constitutive forces of the beam and must be satisfied for all $x \in [0, L]$. Assume further that the constitutive Eqs. (9)–(11) define a stable material. Such material requires Fréchet's derivative of the constitutive matrix with respect to ε, γ, and κ to be positive definite for any triple ε, γ, and κ.

The directional differentiation of constitutive Eqs. (9)–(11) with respect to ε, γ, and κ gives

$$\Delta \mathcal{N}_c = \left(\int_A \frac{\partial \sigma_c}{\partial e} dA \right) \Delta \varepsilon + \left(\int_A z \frac{\partial \sigma_c}{\partial e} dA \right) \Delta \kappa = C_{11} \Delta \varepsilon + C_{13} \Delta \kappa, \tag{34}$$

$$\Delta \mathcal{Q}_c = \left(\int_A \frac{\partial \tau_c}{\partial \gamma} dA \right) \Delta \gamma = C_{22} \Delta \gamma, \tag{35}$$

$$\Delta \mathcal{M}_c = \left(\int_A z \frac{\partial \sigma_c}{\partial e} dA \right) \Delta \varepsilon + \left(\int_A z^2 \frac{\partial \sigma_c}{\partial e} dA \right) \Delta \kappa = C_{31} \Delta \varepsilon + C_{33} \Delta \kappa. \tag{36}$$

Functions $C_{11}(x)$, $C_{13}(x)=C_{31}(x)$, $C_{33}(x)$, and $C_{22}(x)=G(x)A_s$ introduced above are the components of the symmetric tangent constitutive matrix of the cross-section, $C(x)$. C_{11}, C_{13}, and C_{33} are functions of the current distribution of the uniaxial tangent modulus of material in tension and compression, $\partial\sigma_c/\partial e$, while C_{22} is a function of the tangent shear modulus; all of them depend also on cross-sectional geometry. For *stable materials*, C must be positive definite in any cross-section x; this requires its leading principal minors to be positive

$$C_{11}>0, \ C_{11} \ C_{22}>0, \quad \det C=C_{22} \ (C_{11}C_{33}-C_{13}^2)>0. \tag{37}$$

Observe that the second inequality in Eq. (37) can be substituted by the inequality $C_{22}>0$, and the third by the inequality $C_{11}C_{33}-C_{13}^2>0$. When one of the three quantities C_{11}, C_{22} or $\det C/C_{22}$ becomes zero, the cross-section exhibits *material instability*. For materials that do not exhibit softening, it can be shown that whenever C_{11} becomes zero, so do C_{13}, C_{33}, and $\det C$. The material instability is then characterized by a double zero eigenvalue of C. This clustering of zero eigenvalues of material tensor has also been reported by Reese and Wriggers (1997) in the 3D finite elasticity context. Observe also, and as noted by Belytschko and Fish (1989) in the context of strain-softening materials, that zero-valued tangent material modulus, $E_t=\partial\sigma_c/\partial e=0$, in a material point (x, y, z) of the cross-section, is generally not a sufficient condition for the material instability of the supported beam.

Solving Eqs. (6) and (7) for ε and γ functions of κ and boundary parameters $\mathcal{R}_1(0)$, $\mathcal{R}_2(0)$, and $\varphi(0)$ inserting the results into (33) gives

$$r_3^*(\kappa(x), \mathcal{R}_1(0), \mathcal{R}_2(0), \mathcal{M}(0), \varphi(0))= \mathcal{M}_c - \mathcal{M}(0) - \int_0^x \left\{\left[(1+\varepsilon)-\frac{\mathcal{N}}{GA_s}\right]\mathcal{Q}-m_y\right\}d\xi=0. \tag{38}$$

For a set of prescribed boundary parameters, $\mathcal{R}_1(0)$, $\mathcal{R}_2(0)$, $\mathcal{M}(0)$, and $\varphi(0)$, the linearization of Eq. (38) is performed only with respect to κ; the resulting operator must be positive definite in a locally stable state which requires

$$\delta\kappa\frac{d}{d\alpha}r_3^*(\kappa+\alpha\Delta\kappa)|_{\alpha=0} > 0. \tag{39}$$

Inequality (39) also expresses the physically based requirement that the variation of the modified principle of virtual work Eq. (14) is positive definite for arbitrary length L. Upon performing the indicated derivative, we obtain

$$\delta\kappa D \ \Delta\kappa > 0, \tag{40}$$

where

$$D(x) = D_M(x) - D_S(x), \tag{41}$$

and $D_M(x)$ and $D_S(x)$ designate the expressions

$$D_M(x)=C_{33} - \frac{C_{13}^2}{C_{11}}=\overline{C}_{33}, \tag{42}$$

$$D_S(x)=\frac{C_{13}\mathcal{Q}}{C_{11}} \frac{\partial\varphi}{\partial\kappa} - \int_0^x \left[\frac{C_{13}\mathcal{Q}}{C_{11}}+\left(\left(\frac{1}{C_{11}} - \frac{1}{GA_s}\right)\mathcal{Q}^2- (1+\varepsilon)\mathcal{N}+\frac{\mathcal{N}^2}{GA_s}\right)\frac{\partial\varphi}{\partial\kappa}\right] f(\xi)d\xi. \tag{43}$$

Arbitrary function f is defined as $f(\xi) = \Delta\kappa(\xi)/\Delta\kappa(x)$, $|f| \leq 1$. After imposing the requirement of the positive definiteness of D in Eq. (40), and repeating the reformulated inequalities of Eq. (37) as discussed, we obtain the complete set of the necessary and sufficient conditions for the local stability in the beam

$$C_{11} > 0, \quad C_{22} > 0, \quad \bar{C}_{33} > 0, \quad D > 0 \quad \text{for all } x \in [0, L]. \tag{44}$$

The first three inequalities define 'material' stability conditions, and $D > 0$ is a 'structural' stability-type constraint in a local sense.

In a typical Galerkin-type finite element discretization, the local stability conditions as given in (44) are not consistently accounted for in the formulation of the tangent stiffness matrix of an element. As a result, the loss of the local stability does not adequately generate the onset of the global instability.

Observe that D, given by (41), is generally valid for a wide variety of materials, including elastic and hyperelastic ones. It can formally be split into a sum of a pure material part, D_M, and a combined material–stress–resultant part, D_S. In a small strain situation, where the material part dominates, the local stability occurs when material moduli decrease sufficiently, while for large displacements, the local instability may also be stress-triggered. When the tangent constitutive matrix becomes singular at some x, a bifurcation can occur in such a manner that subsequent deformations at x become discontinuous. However, the analysis of this post-bifurcation, 'shear band' phenomenon is beyond the scope of the present paper.

In the next section, we show how the local stability condition $D > 0$ (44) can consistently be incorporated into the element tangent stiffness matrix of the planar beam finite element presented in Section 2 and derive the set of rules for the numerical integration algorithm over the axis of the beam such that the consistency is assured.

4. The consideration of the local stability condition in the planar beam finite element

The basis of our deduction is the finite element beam formulation presented in Section 2.3. To facilitate the analysis of the local stability, we assume that the beam finite element is clamped at one end, and free at the other. Then the loss of the stability of the element coincides with the first appearance of the local instability within the element. As discussed above, the loss of the stability of the element is characterized by the loss of the positive definiteness of its tangent stiffness matrix $\boldsymbol{K_T}$. It can be shown that the determinants of the whole stiffness matrix and of its pseudocurvature-dependent part are linearly related; thus we only need to study the definiteness of the latter. For the present finite element, it takes the form

$$K_{np} = \frac{\partial g_n}{\partial \kappa_p} = \int_0^L D_p P_p P_n \, dx, \quad (n, p = 1, 2, \dots, N), \tag{45}$$

where D_p is given by the equation

$$D_p(x) = \bar{C}_{33} - \frac{1}{P_p}\left\{ \frac{C_{31}\mathcal{Q}}{C_{11}}P_p{}^* - \int_0^L\left[\frac{C_{13}\mathcal{Q}}{C_{11}}P_p + \left(\left(\frac{1}{C_{11}} - \frac{1}{GA_s}\right)\mathcal{Q}^2 - (1+\varepsilon)\mathcal{N} + \frac{\mathcal{N}^2}{GA_s}\right)P_p{}^*\right]d\xi \right\}. \tag{46}$$

As observed, D_p is D from Eq. (41) with f taken to be a specific function $f=P_p$. As required in (44), whenever D_p at some $x_{cr} \in [0, L]$ becomes zero or negative, the local instability takes place at x_{cr} and matrix $[K_{np}]$ must simultaneously become singular or negative definite. The replacement of the integral in (45) with a numerical quadrature gives

$$K_{np}=\sum_{i=1}^{M} w_i D_p(\xi_i) P_p(\xi_i) P_n(\xi_i), \quad (n, p=1, 2, \ldots, N), \tag{47}$$

where positive numbers w_i $(i=1, 2, \cdots, M)$ are the integration weights and M is the number of integration points. Numbers $\xi_i \in [0, L]$ designate the x-coordinates of the i-th integration point. The square matrix $[K_{np}]$ as defined by (47) may be written in the form of a product of three matrices

$$[K_{np}]=\boldsymbol{P}\boldsymbol{W}\boldsymbol{D}_P^t, \tag{48}$$

where $\boldsymbol{P}$ is the rectangular matrix of the values of the polynomials at the integration points

$$P=\begin{bmatrix} P_1(\xi_1) & P_1(\xi_2) & \ldots & P_1(\xi_M) \\ P_2(\xi_1) & P_2(\xi_2) & \ldots & P_2(\xi_M) \\ \vdots & \vdots & \ddots & \vdots \\ P_N(\xi_1) & P_N(\xi_2) & \ldots & P_N(\xi_M) \end{bmatrix}_{N \times M}, \tag{49}$$

$\boldsymbol{W}$ is the diagonal, positive definite matrix of integration weights

$$\boldsymbol{W}=\begin{bmatrix} w_1 & & & 0 \\ & w_2 & & \\ & & \ddots & \\ 0 & & & w_M \end{bmatrix}_{M \times M}, \tag{50}$$

and the rectangular matrix $\boldsymbol{D}_P$ is defined by the expression

$$\boldsymbol{D}_P=\begin{bmatrix} D_1(\xi_1)P_1(\xi_1) & D_1(\xi_2)P_1(\xi_2) & \ldots & D_1(\xi_M)P_1(\xi_M) \\ D_2(\xi_1)P_2(\xi_1) & D_2(\xi_2)P_2(\xi_2) & \ldots & D_2(\xi_M)P_2(\xi_M) \\ \vdots & \vdots & \ddots & \vdots \\ D_N(\xi_1)P_N(\xi_1) & D_N(\xi_2)P_N(\xi_2) & \ldots & D_N(\xi_M)P_N(\xi_M) \end{bmatrix}_{N \times M}. \tag{51}$$

If the number of interpolation nodes is greater than the number of integration points ($N>M$), the rank of matrix $[K_{np}]_{N \times N}$ is at most M and is, thus, always singular, even if all $D_p(\xi_i)>0$. In contrast, if $N<M$, the matrix is generally non-singular even if one of $D_p(\xi_i)$'s is zero. Only if $N=M$ the matrix may–although only under certain conditions–become singular exactly when one of $D_p(\xi_i)$'s vanishes. A special consideration is needed to further establish additional conditions when $N=M$.

When $N=M$, matrices $\boldsymbol{P}$ and $\boldsymbol{D}_P$ become quadratic. The determinant of $[K_{np}]$ is then computed as a product of the determinants of the matrix factors

$$\det[K_{np}]=\det\boldsymbol{P} \det\boldsymbol{W} \det\boldsymbol{D}_P^t. \tag{52}$$

Because M interpolation polynomials of degree $M-1$ are linearly independent and continuous functions, it can be proved that the first determinant on the right-hand side of (52) is always positive, i.e., det $\boldsymbol{P}>0$. Likewise is true for det $\boldsymbol{W}$. The sign of det $[K_{np}]$ then solely depends on the sign of det $\boldsymbol{D}_P$:

$$\text{sgn}(\det[K_{np}]) = \text{sgn}(\det \boldsymbol{D}_P) =$$

$$\text{sgn}\begin{bmatrix} D_1(\xi_1)P_1(\xi_1) & D_1(\xi_2)P_1(\xi_2) & \ldots & D_1(\xi_M)P_1(\xi_M) \\ D_2(\xi_1)P_2(\xi_1) & D_2(\xi_2)P_2(\xi_2) & \ldots & D_2(\xi_M)P_2(\xi_M) \\ \vdots & \vdots & \ddots & \vdots \\ D_M(\xi_1)P_M(\xi_1) & D_M(\xi_2)P_M(\xi_2) & \ldots & D_M(\xi_M)P_M(\xi_M) \end{bmatrix}. \tag{53}$$

We seek a combination of a numerical integration scheme and an interpolation that yields zero determinant whenever one of $D_i(\xi_j)$'s becomes zero. For the sake of simplicity of discussion, but without losing generality, we accept that the local stability is lost in integration point one, then $D_1(\xi_1)=0$. There are a variety of possible solutions. If we employ equidistant interpolation nodes with Lagrangian interpolation polynomials in combination with the Newton-Cotes integration rule with the integration points coinciding with the interpolation nodes, then $P_1(\xi_1)=1$ and $P_1(\xi_2)=P_1(\xi_3)=\cdots=P_1(\xi_M)=0$. The first row in Eq. (53) then vanishes if $D_1(\xi_1)=0$, and so does the determinant. We here advise a more practical and simple approach which causes in the first column to vanish. We require that interpolation polynomials other than polynomial P_1 are zero in integration point one, i.e. $P_i(\xi_1)=0$ ($i=2, 3, \cdots, M$). This condition essentially demands that both the first interpolation node and the first integration point, are located at the point of the local instability. Such a condition is automatically satisfied for the two boundary nodes when the Lagrangian interpolation in conjunction with Lobatto's integration is employed.

Therefore, Eq. (52) reduces to

$$\det[K_{np}] = D_1(\xi_1)\, \det\boldsymbol{P}\, \det\boldsymbol{W}\, \det[\boldsymbol{D}_P^t]_{M-1 \times M-1}, \tag{54}$$

where $[\boldsymbol{D}_P^t]_{M-1 \times M-1}$ is a ($M-1$)-dimensional submatrix of $\boldsymbol{D}_P^t$. As observed from (54), the determinant of the tangent stiffness matrix is now proportional to $D_1(\xi_1)$.

Unfortunately, the point of local instability is in general not coincident with an integration point of any standard numerical integration rule (such as, e.g., Simpson's, Gaussian, and Lobatto's rules). Thus, in order to capture the onset of the local instability correctly, one has (i) to detect the point of the local instability on the axis of the beam, (ii) to collocate the interpolation, the integration and the instability points, and (iii) to construct proper interpolation functions and a customized integration rule. This, a rather complicated procedure, may in practice be largely avoided, because local instabilities usually occur at the two end points of the finite element; therefore, the Lagrangian interpolation with the set of equidistant nodes (which includes the two end points) combined with standard Lobatto's integration, suffices. Lobatto's formulae have been used extensively in practical elastic-plastic analyses, see, e.g., Banovec (1986), Bergan (1984), Cichoń (1984), Hsiao *et al.* (1988), and Saje *et al.* (1997).

Remark 4.1. The derivation indicates that taking an order of numerical integration higher than deduced above ($M > N$) gives the determinant greater results than expected which induces in an overstiff response and an overestimation of the global instability load. This will be confirmed by numerical experiments. An exception occurs, however, if an element is subjected to a homogeneous bending, where all $D_p(\xi)$'s become zero simultaneously along the beam.

Remark 4.2. For the small deformation theory (the so called 1st order theory) matrix $[K_{np}]$ again takes a form of a triple matrix product

$$[K_{np}] = \boldsymbol{P}\bar{\boldsymbol{C}}_w\boldsymbol{P}^t, \tag{55}$$

but the deduction and the results are now more simple due to the diagonal form of matrix $\overline{C}_w$:

$$\overline{C}_w = \begin{bmatrix} w_1\overline{C}_{33}(\xi_1) & & & 0 \\ & w_2\overline{C}_{33}(\xi_2) & & \\ & & \ddots & \\ 0 & & & w_M\overline{C}_{33}(\xi_M) \end{bmatrix}_{M \times M} . \tag{56}$$

Here, the local stability condition reduces to $\overline{C}_{33} = C_{33} - C_{13}^2/C_{11} > 0$. Since det $\boldsymbol{P} > 0$, matrix $[K_{np}]$ becomes singular when one of the $\overline{C}_{33}(\xi_i)$'s becomes zero, provided, however, that $N=M$. This is a lot less restrictive condition than that appearing in the finite deformation case, where interpolation, integration and instability points must coalesce. Fully analogous results have been derived by Banovec (1986) for his mixed-energy based, moderate-rotations, co-rotational, elastic-plastic beam element, and Saje *et al.* (1997) for their exact-kinematics, rotation-based, elastic-plastic beam finite element.

Remark 4.3. It is clear from (52) that the proposed integration technology guarantees that the value of the determinant of the tangent stiffness matrix in the neighbourhood of the critical point decreases with the determinant of $\boldsymbol{D}_P^t$. Moreover, Eq. (54) shows that det $\boldsymbol{K}_T$ is proportional to $D_p(\xi_{cr})$. Thus, both the determinant of the tangent stiffness matrix and $D_p(\xi_{cr})$ approach zero linearly. This fact is essential for the appropriate numerical accuracy of the incremental solution in the vicinity of the singular or instability point, where substantial changes in deformations should result from small load increments. This also suggests that the accuracy of the evaluation of the residual forces is essential in the neighbourhood of the singular point.

Remark 4.4. The lowest reasonable order of numerical integration of the finite elements described in Section 2.3 can be estimated by requiring that the integral in (45) shall be integrated exactly for a materially and geometrically linear case, when D_p can be assumed constant as in Jelenić and Saje (1995) for the elastic, rotation-based space beam model. Then its integrand appears to be the polynomial of degree $2(N-1)$. An exact integration of this polynomial is possible by, e.g., the N-point Gaussian, the N-point Lobatto-like integration with only one integration point prescribed in advance, and the $(N+1)$-point classical Lobatto's integration. For a linear elastic case, Gaussian integration is obviously optimal. In contrast, for the capturing of the local-global stability relation consistently, the use of the Lobatto-like integration with only one prescribed integration point (this one being the local stability point) is essential.

Remark 4.5. Notice from Eq. (46) that $D_p = \overline{C}_{33}$ at $x=0$ and $x=L$.

5. Numerical examples

To show the validity of the present theoretical results and to give an estimate of the errors possibly made when the local stability conditions are not accounted for properly, we consider two numerical examples: (i) a rather flexible elastic-plastic cantilever subjected to a transverse point load, and (ii) a simply supported beam subjected to a transverse uniform load and/or an axial point load at the support.

Elastic-plastic material is assumed whose uniaxial stress-strain law is taken to be represented by a bi-linear rule of the form

$$\sigma_c(e) = \begin{cases} Ee, & |e| < e_Y \\ (\sigma_Y + E_p(|e| - e_Y))\operatorname{sgn}(e), & |e| \geq e_Y \end{cases}. \tag{57}$$

Parameter $E > 0$ is the elastic, and $E_p \geq 0$ is the plastic tangent modulus of material; $\sigma_Y = Ee_Y > 0$ is the yield stress, and $e_Y > 0$ denotes the yield extensional strain. In what follows, we consider the numerically most demanding case–elastic–perfectly plastic material ($E_p = 0$). Note that the law, given by (57), enables the exact analytical integration over the cross-section.

The influence of various integration schemes on the local-global stability relation is studied using finite elements of Saje *et al.* (1997) with various degrees of interpolation polynomials for the rotation approximation and different types and orders of the numerical integration. These finite elements are designated by $E_{\text{i-n}}$, where the first subscript, 'i', specifies the degree of the rotational interpolation polynomial, and subscript 'n' determines the order of the numerical integration.

5.1 Flexible cantilever

The descriptive geometric, material, and loading data are given in Fig. 1. We study a very slender cantilever beam with a large length-to-height ratio, $L/h = 50$, which makes the effect known as shear negligible. The rectangular cross-section is assumed with the width-to-height ratio 1/4.

With an increasing load, the plastic zone localizes at the clamped cross-section. When the clamped cross-section is sufficiently plastified, the cantilever loses its stability. The instability is materially dominant. As the clamped end is the potential point of the local instability, it must be taken to be both the interpolation and the integration point. Lobatto's integration rule satisfies this requirement, but not the Gaussian.

For the purpose of comparison of various results, we first constructed several numerical solutions using uniform meshes of one, ten, and twenty, Lobatto's consistent integration-based elements E_{5-5}, and compared the solutions for the geometrical, deformation, and stress quantities. We found relative differences to be less than 10^{-3} between the ten- and twenty-element solutions. The twenty-element solution thus appears to be sufficiently accurate and is, therefore, chosen as the reference solution in the subsequent analyses; in the sequel, it will be marked as 'exact' solution.

Fig. 2a shows the non-dimensional force–tip deflection diagrams as predicted by twenty-element uniform meshes using (i) element E_{5-5} and Lobatto's integration with the consistent number of integration points, and (ii) element E_{5-7} with an inconsistent number of points, yet with the correct location of the first point. The localized plastic zone makes the cantilever rather flexible. The results are shown for the range $w/L \in [0, 0.36]$. As seen from the figure, 20-element E_{5-7} solution exhibits a slightly smaller tip deflection for $\lambda > 4$ than the solution that employs E_{5-5}. This shows that the influence of a solely inconsistent numerical integration order is not very pronounced when the
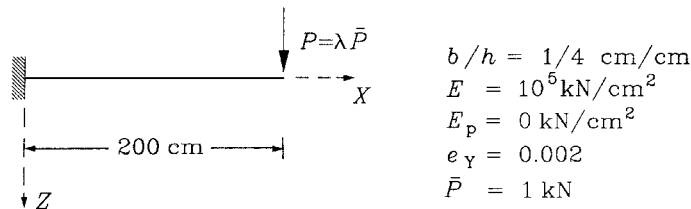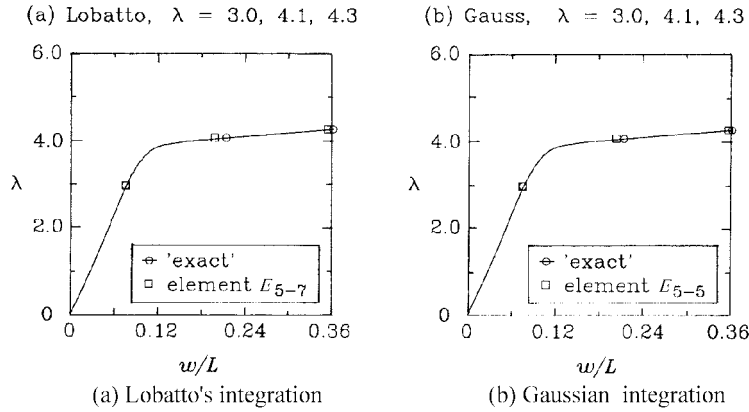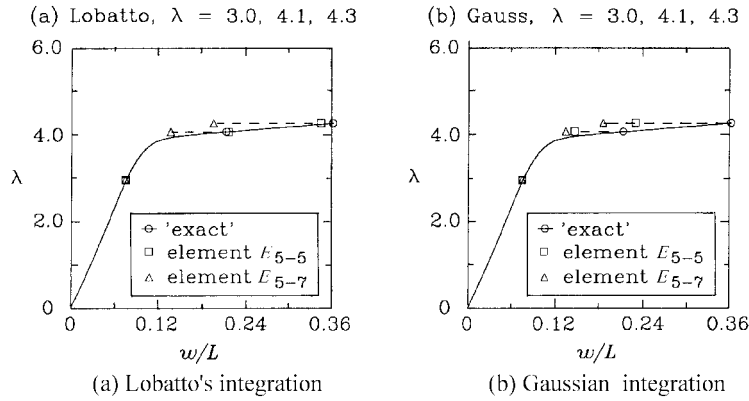

Fig. 1 A cantilever subjected to transverse point load P

(a) Lobatto's integration   (b) Gaussian integration

Fig. 2 Force–tip deflection diagrams, 20 elements $E_{5\text{-}5}$ ('exact' solution) or $E_{5\text{-}7}$

(a) Lobatto's integration   (b) Gaussian integration

Fig. 3 Force–tip deflection diagrams, one element $E_{5\text{-}5}$ or $E_{5\text{-}7}$

number of elements is sufficiently large. The use of the Gaussian integration with a consistent number of points but with an inconsistent location of the first point gives the results that show the same trend (Fig. 2b).

Fig. 3 shows the non-dimensional force-tip deflection diagrams as predicted by one-element meshes using elements $E_{5\text{-}5}$ and $E_{5\text{-}7}$ with Lobatto's (Fig. 3a) and Gaussian (Fig. 3b) integrations. The figures clearly show (i) that an inconsistent Lobatto's or Gaussian numerical integrations ($E_{5\text{-}7}$) lead to an overestimation of the bearing capacity of the cantilever, although for the present numerical example absolute errors in the load are relatively small; and (ii) that the tip deflections for a prescribed load are significantly smaller when the inconsistent integration is used.

This is further demonstrated by Fig. 4, where the deformed shapes of the cantilever for λ=4.3 are shown for one-element $E_{5\text{-}5}$ and $E_{5\text{-}7}$ meshes using Lobatto's (Fig. 4a) or Gaussian integration (Fig. 4b) and compared to the 'exact' solution. The comparison shows that the deflections obtained by the inconsistent integration are roughly one half of the correct values, while the consistent integration results in practically accurate deflections.

The cause for the underestimation of the deflections is inability of the inconsistent integration solutions to predict a sufficient localization of the pseudocurvature at a clamped section. Fig. 5

(a) Lobatto's integration   (b) Gaussian integration
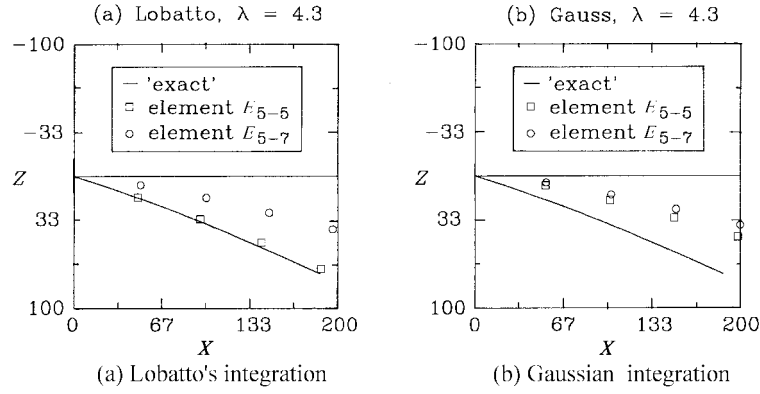
Fig. 4 Deformed shapes at $\lambda = 4.3$, one element $E_{5\text{-}5}$ or $E_{5\text{-}7}$
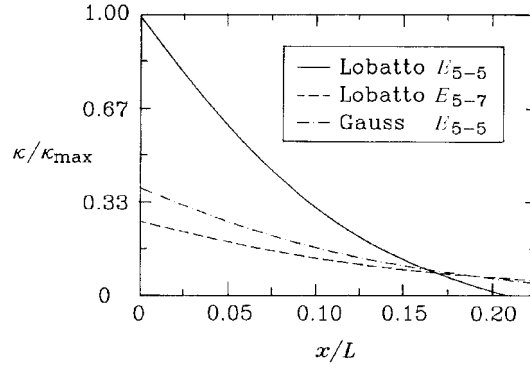
Fig. 5 Variation of the pseudocurvature, κ, with x at $\lambda = 4.3$, one-element mesh

shows the graph of the curvature variation along the cantilever for a one-element mesh. Note that the application of the consistent integration predicts about the three times bigger localization.

5.2 Simply supported beam

The geometric, material, and loading data are given in Fig. 6. Again, the effect of shear is taken to be negligible. For convenience, the combined load is defined by

$$F(\alpha) = \lambda((1-\alpha)\bar{q} + \alpha\bar{P}),\qquad(58)$$

where λ is the loading factor, applied to the reference distributed load $\bar{q}$, and the point load $\bar{P}$; $\alpha \in$ [0, 1] is a parameter. When $\alpha=0$, the beam bends and the instability stems from the spread material; plasticity we call this case a 'materially dominant instability'; in contrast, for $\alpha=1$ the stability is lost by buckling and is, therefore, 'geometrically dominant'.

Materially Dominant Instability. We study the materially dominant instability first. Since the beam is now subjected to the transverse load $q=\lambda\bar{q}$, the plastic zone will localize at the center point of the beam. For the consistent consideration of local instability, an interpolation point and an integration point should be situated at the center point. The condition is met when (i) Lobatto's or Gaussian integration of an odd order is used, or (ii) such that the end node of an element coincides

$$b/h = 1/4 \text{ cm/cm}$$
$$E = 1.2 \ 10^5 \text{ kN/cm}^2$$
$$E_{\mathrm{p}} = 0 \text{ kN/cm}^2$$
$$e_{\mathrm{Y}} = 0.0012$$
$$\bar{P} = 1 \text{ kN}$$
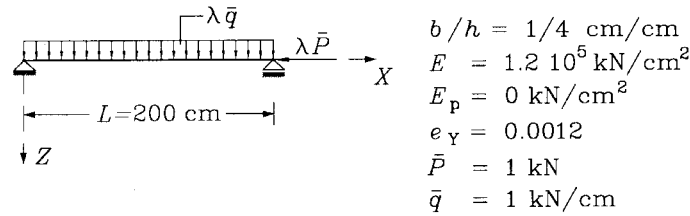$$\bar{q} = 1 \text{ kN/cm}$$

Fig. 6 Simply supported beam

with the center point if the beam is modelled by several finite elements; in the latter case, only Lobatto's integration (but of an arbitrary order) is consistent. From these considerations and recalling the results of Section 5.1, it is obvious that Lobatto's integration is a better choice. Therefore, in what follows, we show only results using Lobatto's integration.

We first obtained a series of numerical solutions using uniform meshes of one, ten, and twenty Lobatto's consistent integration-based elements $E_{9\text{-}9}$, and compared the solutions. We found relative differences between geometrical, deformation, and stress quantities to be less than $5 \cdot 10^{-3}$ for ten and twenty-element solutions. The twenty-element solution is chosen as the reference solution; in figures, it is marked as 'exact' solution.

Fig. 7a shows the loading factor-mid-point deflection diagrams as predicted by twenty-element uniform meshes using (i) consistent element $E_{9\text{-}9}$, and (ii) inconsistent element $E_{5\text{-}7}$. Fig. 7a shows that the differences are small, and indicates that the influence of an inconsistent order of integration diminishes when the number of elements grows. In contrast, when only one-element mesh is employed, the inconsistent elements $E_{6\text{-}6}$ and $E_{5\text{-}7}$ give roughly three times smaller deflections, compared to our reference solution. The consistent element $E_{5\text{-}5}$, on the other hand, gives nearly accurate results for deflections.

This is further illustrated by Fig. 8, where the deformed shapes of the simply supported beam for $\lambda = 0.12$ are shown for one-element $E_{5\text{-}5}$, $E_{5\text{-}7}$, and $E_{6\text{-}6}$ meshes and compared to the deformed shape obtained by the 'exact' solution. Note that element $E_{6\text{-}6}$ has the correct order of integration, but is inconsistent because the order is not an odd number. Observe also that the error in deflections due to the inconsistency is now even bigger than found in the example in Section 5.1 (the factor is here

(a) 20 elements $E_{9\text{-}9}$ ('exact' solution) or $E_{5\text{-}7}$ (b) one element $E_{5\text{-}5}$, $E_{5\text{-}7}$ or $E_{6\text{-}6}$
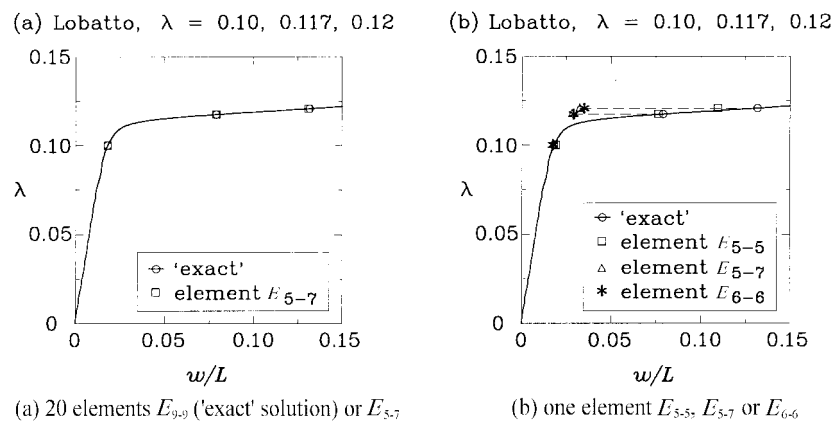
Fig. 7 Force–tip deflection diagrams, $\alpha = 0$
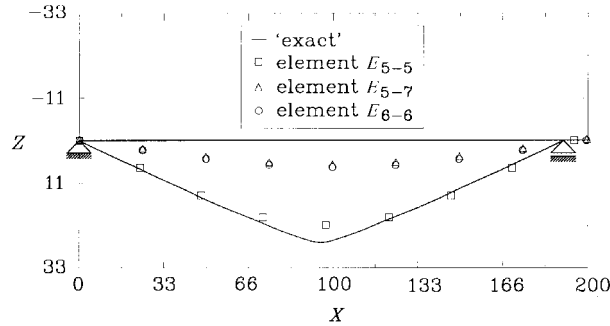
Fig. 8 Deformed shapes at $\lambda=0.12$–Lobatto's integration; $\alpha=0$, one element $E_{5\text{-}5}$, $E_{5\text{-}7}$ or $E_{6\text{-}6}$

about 4 compared to 2 in Sec. 5.1). Both examples indicate that the inconsistent elements of type $E_{n\text{-}m}$, m $\geq$ n, yield too stiff tangent matrices.

Fig. 9 shows the graph of the variation of the pseudocurvature along the axis of the beam. Again, the quantitative differences between the results of consistent element, $E_{5\text{-}5}$, and inconsistent elements, $E_{5\text{-}7}$ and $E_{6\text{-}6}$, are remarkable. Both solution graphs also differ qualitatively: while the graph obtained by element $E_{5\text{-}5}$ exhibits a trend towards the localization, the graphs of $E_{5\text{-}7}$ and $E_{6\text{-}6}$ do not.

The pseudocurvature (and the extensional strain) serves to compute the constitutive bending moment in the beam. Thus, the error in the pseudocurvature results in the error of the bending moment. This is demonstrated by Fig. 10. The inconsistent elements $E_{5\text{-}7}$ and $E_{6\text{-}6}$ yield several times more substantial relative errors compared to the errors of element $E_{5\text{-}5}$.

Geometrically Dominant Instability. The beam is subjected (i) solely to a compressive axial force P (i.e., $\alpha=0$), and (ii) to a combined load with $\alpha=0.9999$. The computed values of critical loading factors λ_{cr} for various element types and number of elements are presented in Table 1. As observed from Table 1, the inconsistency of elements do not play a significant role in the determination of the critical load.

6. Conclusions

In standard finite element algorithms, the local stability conditions are not consistently accounted
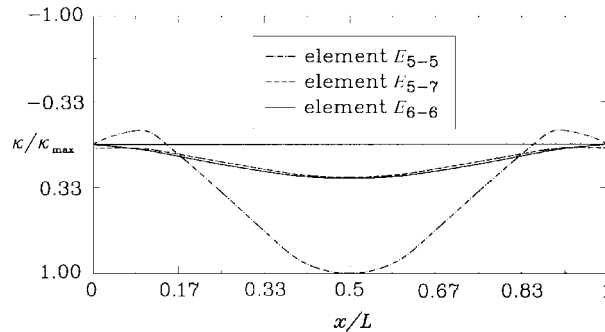

Fig. 9 One-element mesh–Lobatto's integration; $\alpha=0$, variation of the pseudocurvature, κ, with x at $\lambda=0.12$
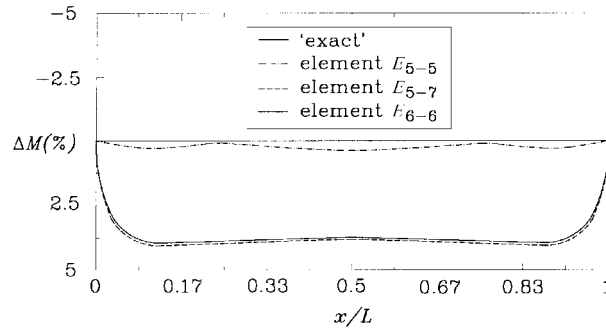
Fig. 10 Variation of the relative error of the bending moment, $\Delta M(\%)=100\ (\mathcal{M}-\mathcal{M}_{\text{exact}})/\mathcal{M}_{\text{exact}}$, with x at $\lambda=0.12$; $\alpha=0$; Lobatto's integration

Table 1 Global stability of the simply supported beam-λ_{cr}; Lobatto's integration

	$\alpha=1$		$\alpha=0.9999$	
	20 elements	one element	20 elements	one element
$E_{5\text{-}5}$	157.966	158.054	127.866	127.311
$E_{5\text{-}7}$	157.966	157.966	127.866	127.705
$E_{6\text{-}6}$	157.966	157.963	127.866	128.634
$E_{9\text{-}9}$	157.966	157.966	127.866	127.937

for in the formulation of the tangent stiffness matrix. As a result, the loss of the local stability is not adequately related to the onset of the global instability. The phenomenon typically arises with material-type localizations, such as shear bands and plastic hinges. This paper addresses the problem in the context of the planar, finite-strain, rate-independent, materially nonlinear beam theory, although the proposed technology is in principle not limited to beam structures.

To make the stability analysis more transparent, we first presented a weak formulation of Reissner's finite-strain beam theory, where the pseudocurvature of the deformed axis plays a role of the only unknown function. Next, we derived the local stability conditions for the large deformation case, and suggested possible combinations of the interpolation and numerical integration schemes that trigger the simultaneous loss of the local and global stabilities of a statically determined finite element. For practical applications, we advised a procedure that uses a special numerical integration rule, where interpolation nodes and integration points equal in number, but not in locations, except for the point of the local instability, where the interpolation point and the integration node coalesce.

The previously derived large-displacement elastic-plastic beam formulations by Banovec (1986) and by Saje *et al.* (1997) employ a similar integration strategy but are based solely on small-strain material instability conditions. As a result, those procedures also require certain relation between a number of interpolation and integration points, but do not additionally set the condition that the interpolation node, the integration point, and the point of the local instability coincide, which is the implication of the present procedure.

In general, the point of local instability is not a priori located in an integration point or in an interpolation node. To fulfill the requirement of the coalescence of the three points, a special algorithm must be used whose essential part is the update of interpolation functions and the construction of a customized integration rule. The details of these issues, however, were not the

subject of this paper. Provided that the point of instability is an end-point of a beam–a condition often met in engineering practice–the algorithm simplifies substantially; one such algorithm uses the Lagrangian interpolation and Lobatto's integration as in Banovec (1986) and Saje *et al.* (1997).

Acknowledgements

References

Antman, S.S., and Rosenfeld, G. (1978), "Global behavior of buckled states of non-linearly elastic rods", SIAM Review, **20**, 513-566.

Banovec, J. (1986), "Geometric and material nonlinear analysis of planar frames", Ph. D. Thesis (in Slovenian), University of Ljubljana, Slovenia.

Belytschko, T., Fish, J., and Engelmann, B.E. (1988), "A finite element with embedded localization zone", *Comput. Meth. in Appl. Mech. and Eng.*, **70**, 59-89.

Belytschko, T., and Fish, J. (1989), "Embedded hinge lines for plate elements", *Comput. Meth. in Appl. Mech. and Eng.*, **76**, 67-86.

Bergan, P.G. (1984), "Some aspects of interpolation and integration in nonlinear finite element analysis of reinforced concrete structures", *Computer Aided Analysis and Design of Concrete Structures*, Part 1, Damjanić, F. *et al.*, eds., Pineridge Press, Swansea, 301-316.

Cichoń, C. (1984), "Large displacements in-plane analysis of elastic-plastic frames", *Comput. and Struct.*, **19**, 737-745.

Cowper, G.R. (1966), "The shear coefficient in Timoshenko's beam theory", *ASME J. Appl. Mech.*, **33**, 335-340.

Crisfield, M.A. (1991, 1997), *Non-linear Finite Element Analysis of Solids and Structures*, Volumes 1 and 2, John Wiley Sons, Chichester.

de Borst, R., Sluys, L.J., Mühlhaus, H.-B., and Pamin, P. (1993), "Fundamental issues in finite element analysis of localization of deformation", *Eng. Comput.*, **10**, 99-121.

Fujii, F., and Okazawa, S. (1997), "Bypass, homotopy path and local iteration to compute the stability point", *Struct. Eng. and Mech.*, **5**, 577-586.

Hohn, F.E. (1973), *Elementary Matrix Algebra*, 3rd edn., The Macmillan Company, New York.

Hsiao, K.M., Hou, F.Y., and Spiliopoulos, K.V. (1988), "Large displacement analysis of elasto-plastic frames", *Comput. Meth. in Appl. Mech. and Eng.*, **28**, 627-633.

Hughes, T.J., and Pister, K.S. (1978), "Consistent linearization in mechanics of solids and structures", *Comput. and Struct.*, **8**, 391-397.

Jelenić, G., and Saje, M. (1995), "A kinematically exact space finite strain beam model–Finite element formulation by generalized virtual work principle", *Comput. Meth. in Appl. Mech. and Eng.*, **120**, 131-161.

Ortiz, M., Leroy, Y., and Needleman, A. (1987), "A finite element method for localized failure analysis", *Comput. Meth. in Appl. Mech. and Eng.*, **61**, 189-214.

Planinc, I. (1998), "A quadratically convergent algorithms for the computation of stability points: the application of the determinant of the tangent stiffness matrix", Ph.D. Thesis (in Slovenian), University of Ljubljana, Slovenia.

Planinc, I., and Saje, M. (1998), "A quadratically convergent algorithm for the computation of stability points: the application of the determinant of the tangent stiffness matrix", *Comput. Meth. in Appl. Mech. and Eng.*, **169**, 89-105.

Reissner, E. (1972), "On one-dimensional finite-strain beam theory: the plane problem", *J. Appl. Math. and Physics* (*ZAMP*), **23**, 795-804.

Reese, S., and Wriggers, P. (1997), "Material instabilities of an incompressible elastic cube under triaxial tension", *Int. J. Solids and Struct.*, **34**, 3433-3454.

Saje, M., Planinc, I., Turk, G., and Vratanar, B. (1997), "A kinematically exact finite element formulation of planar elastic-plastic frames", *Comput. Meth. in Appl. Mech. and Eng.*, **144**, 125-151.

Ting, T.C.T. (1996), "Positive definiteness of anisotropic elastic constants", *Mathematics and Mechanics of Solids*, **1**, 301-314.

Washizu, K. (1981), *Variational Methods in Elasticity and Plasticity*, Pergamon Press, Oxford.

Waszczyszyn, Z., Cichoń, C., and Radwańska, M. (1994), *Stability of Structures by Finite Element Methods*, Elsevier Science B. V., Amsterdam.

Wriggers, P., and Simo, J.C. (1990), "A general procedure for the direct computation of turning and bifurcation points", *Int. J. Numer. Meth. in Eng.*, **30**, 155-176.

Wriggers, P., Wagner, W., and Miehe, C. (1988), "A quadratically convergent procedure for the calculation of stability points in finite element analysis", *Comput. Meth. in Appl. Mech. and Eng.*, **70**, 329-347.